# FITTING NETWORKS MODELS FOR FUNCTIONAL BRAIN CONNECTIVITY

*Jagath C. Rajapakse, Sukrit Gupta, Xiuchao Sui*

School of Computer Science & Engineering
Nanyang Technological University, Singapore

## ABSTRACT

Functional connectivity of the human brain and the hierarchical modular architecture of functional networks can be investigated using functional magnetic resonance imaging (fMRI). Various network models, such as power-law networks and modular networks have been explored before to study brain networks. In order to investigate the plausibility of modeling functional brain networks with network models based on distribution of node degree and connection weights, we will compute the goodness-of-fit of several network models on resting-state fMRI scans gathered in the Human Connectome Project. Our experiments suggest that the power-law networks and stochastic block models aptly fit functional connectivity of the subjects and the stochastic block models have the potential to detect functional modules of the brain.

***Index Terms—*** functional brain networks, functional MRI, model fitting, power-law networks, stochastic block models

## 1. INTRODUCTION

The human brain is a massive neural network whose emerging computations result in adaptive cognition and behavior. Neighboring neurons in the cortex have similar functions and form functionally distinct regions leading to cortical functional parcels. Finding functional parcellations of the brain is currently a topic of intense research [1]. There are increasing evidences to suggest that the functional architecture of the brain is organized in a hierarchical modular manner [2, 3]. The hierarchical modular architecture has evolved due to the need of efficient, low cost information transfer among different brain regions.

Functional magnetic resonance imaging (fMRI) provides an opportunity for *in vivo* investigation of the functional architecture of the brain. Functional connectivity of the human brain is measured by the correlations of time-series of neuronal responses between brain regions and is derived from fMRI images taken at rest or while performing a task. Recent advances in network science provide models and tools to derive brain's functional architecture from functional connectivity obtained from fMRI [4]. Network models such as scale-free networks [6, 7] and modular networks [8, 9, 10] have been used to explore the functional architecture of the brain. Highly connected nodes or hubs that are associated with brain disorders and network modules that correspond to known functional modules of the brain have been identified [4].

In this paper, as models of functional brain networks, we investigate two types of networks: (i) networks that are defined by their degree distributions such as power-law networks, exponential networks, and stretched exponential networks; and (ii) networks that are defined by the distribution of connectivity weights such as standard stochastic block models (SBM) and degree-corrected SBM (dc-SBM). Nervous system has evolved to conserve two themes of wiring [5]: (a) the tendency to organize network topology into modules that serve specialized functionality; and (b) the general drive to high topological integration by means of short communication paths, hubs and rich hubs. We hypothesize that theme (a) of wiring is represented in network models (ii), namely stochastic block models, and theme (b) of wiring is represented in network models (i) defined with node distributions.

By using resting-state fMRI (rs-fMRI) brain scans collected in the Human Connectome Project [1] [12], we will evaluate the goodness-of-fit of several network models touted for modeling functional brain connectivity. We will first investigate the power-law and exponential network models which are characterized by nodal connectivity and then use stochastic block models to unfold the functional modules of the brain. We will show that the power-law and exponential models fit well on functional brain networks and demonstrate the potential of stochastic block models in detecting functional modules of the brain [11, 13, 14]. In order to reduce the complexity, we used functional connectivity among 264 regions of interests (ROI) identified by Power et al. as functionally relevant cortical regions [15].

## 2. METHODS

### 2.1. Models of Brain Connectivity

We consider the functional network of the brain as a graph $G$ of $n$ brain nodes or regions of interests (ROI). Let $W = \{w_{ij}\}$ denote the functional connectivity matrix or the adjacency

[1] db.humanconnectome.org

978-1-5090-1172-8/17/$31.00 ©2017 IEEE

matrix of the brain where $w_{ij} \in \{0,1\}$, and $k_i = \sum_j w_{ij}$ denote the degree of $i$th node.

The functional architecture of the brain is studied by fitting network models to functional connectivity of the brain. We consider five network models to fit into the functional connectivity of brain: power-law network model, exponential model, stretched exponential model, standard random block model and degree-corrected random block model.

#### *2.1.1. Power-law and Exponential Networks*

A power-law network is defined by the nodal degree ($k$) distribution [16, 17]:

$$p_{\text{power}}(k) = C_1 k^{-\alpha}$$

where $\alpha$ is the scaling parameter, $C_1 = (\alpha - 1)\, k_{\min}^{\alpha-1}$, and $k_{\min}$ is the minimum degree that obeys the power-law.

The networks with exponential degree distribution are defined by [17]

$$p_{\text{exponential}}(k) = C_2 \exp(-\lambda k)$$

where $\lambda$ is the decay parameter and $C_2 = \lambda \exp(\lambda k_{\min})$.

The stretched exponential networks combine power-law and exponential degree distributions and are defined by [18, 17]:

$$p_{\text{stretched}}(k) = C_3 k^{\beta-1} \exp\left(-\lambda k^{\beta}\right)$$

where $C_3 = \beta\lambda \exp\left(\lambda k_{\min}^{\beta}\right)$ and $\lambda$ is the decay parameter.

#### *2.1.2. Stochastic Block Models*

Stochastic block models (SBM) partition the set of nodes into modules (or clusters) with many intra-modular edges and few inter-modular edges. Suppose that the block model partitions the brain network $G$ into a set of modules, $M = \{M_i\}$ where $M_i$ denotes the index of the module of node $i$. Let $E = \{e_{rs}\}$ where $e_{rs}$ denotes the expected number of edges between nodes $i$ and $j$ belonging to modules $r$ and $s$.

The stochastic block model is defined by a Poisson distribution of edges.The likelihood of $G$ of the standard stochastic block model (SBM) is given by [11]:

$$p_{\text{SBM}}(G|E,M) = \frac{1}{\prod_{i<j} w_{ij}!} \prod_{r,s} e_{rs}^{\frac{m_{rs}}{2}} \exp(-n_r n_s e_{rs})$$

where $m_{rs} = \sum_{i,j,M_i=r,M_j=s} w_{ij}$ and $n_r$ is the number of nodes in module $r$.

A degree-corrected stochastic block models (dc-SBM) was introduced to account for the degree distribution of edges, which is given by [11]:

$$p_{\text{dc-SBM}}(G|E,M) = \frac{1}{\prod_{i<j} w_{ij}!} \prod_i \theta_i^{k_i} \prod_{r,s} e_{rs}^{\frac{m_{rs}}{2}} \exp\left(-\frac{e_{rs}}{2}\right)$$

where $\theta_i$ is normalizing parameter such that $\sum_{i,M_i=r} \theta_i = 1$ and $k_i$ denote the degree of node $i$.

### 2.2. Model Fitting

In order to find the plausibility of different network models, we first fit different models on functional connectivity matrices evaluated on subjects. For each subject, average time-series of brain voxels within a sphere of 5mm radius at the 264 functionally relevant ROI defined in [15] were obtained. Functional connectivity of the brain is obtained by calculating partial correlations between resting-state fMRI time-series of the ROIs. We discarded negative edges and thresholded the functional connectivity for a range of thresholds in order to investigate the functional architecture of the brain. We consider unweighted networks with connectivity matrix $W$ for model fitting.

For power-law and exponential networks, the parameters $\{x_{\min}, \alpha, \beta, \lambda\}$ were estimated by using KS statistics and maximum likelihood estimates as described in [17]. For stochastic block models, the parameters were estimated by minimizing the description length of the model as described in [14].

## 3. RESULTS

### 3.1. Data

The dataset included 627 healthy adults from ages 22-36 from the S900 release of the HCP. All HCP rs-fMRI data were acquired on a Siemens Skyra 3T scanner at the Washington University. The details of MR imaging protocols are described in the S900 release manual available at HCP website. We used preprocessed data that had undergone standard preprocessing steps [20] and subsequent ICA-denoising [21] in order to remove artifacts and noises. In addition, 24 head motion parameters were regressed out of the time series.

### 3.2. Goodness-of-Fit

Connectivity matrices of individual subjects were the data points for network analysis. Each subject's data was fitted with power-law, exponential, and stretched exponential (stretched) distributions and standard and degree-corrected SBM. The power-law and exponential models were implemented using the power-law python package [19]. The standard and degree-corrected random block models were implemented by using the graph-tool package [24].

The goodness-of-fit values of each subject scan to different models were evaluated by computing the log likelihood values given the models. The averages of log likelihoods on all subjects for each model at different thresholds of connectivity are given in figure 1. As seen, the stretched exponential had the highest likelihood, so the best fitting. The power-law and exponential networks attempt to fit the corresponding degree distribution to the data while stochastic block models attempt to fit distributions of connections to brain networks.

**Table 1**: Standard Deviation in log likelihood of different models computed on all scans at different threshold values $w_0$ of functional connectivity.

| Standard Deviation ($\sigma$) | $w_0$ = 1.2 | $w_0$ = 1.6 | $w_0$ = 2.0 | $w_0$ = 2.4 |
|---|---|---|---|---|
| Exponential | 41.3 | 62.4 | 123.9 | 101.9 |
| Power-law | 33.3 | 52.5 | 130.7 | 105.2 |
| Stretched | 31.1 | 53.4 | 122.9 | 100.9 |
| dc-SBM | 467.6 | 387.7 | 317.2 | 258.1 |
| SBM | 460.8 | 381.4 | 312.2 | 256.3 |

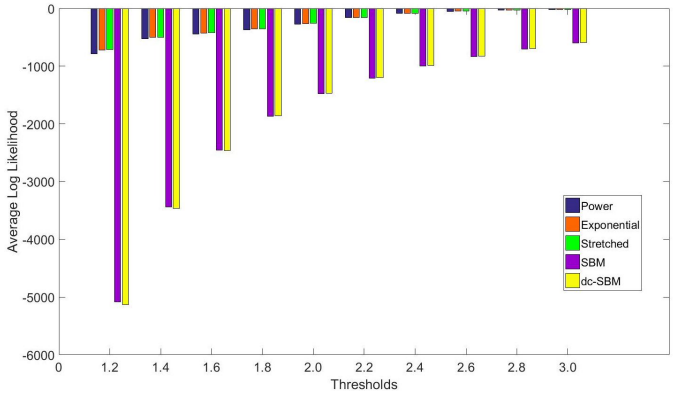


**Fig. 1**: Average log-likelihoods of all the subjects by different models at different threshold values of connectivity.

Figure 2 shows connectivity network for a representative subject at different thresholds. The number of connections reduce as the connectivity threshold is increased. 1 gives us the standard deviation in the log likelihood values across all subjects for different models and threshold values.

### 3.3. Comparison of Models

In order to compare different models, we compute log likelihood ratios between two models and corresponding p-values, which are shown in Table 2. We assumed each subject to be a data sample and calculated the p-values by computing the average and standard deviation of the log likelihood ratios as described in [23]. As seen, the model fits were significantly different from one another ( $p < 0.05$ ) and capture different aspects of the functional architecture.

### 3.4. Functional Modules

We calculated the modules by using both standard and degree-corrected stochastic block models. Since the quality of fit for random block models depends on initial parameters, we chose the best fit over 25 random initializations . The modules detected for a representative subject by stochastic block models are shown in figure 3. The variation of the number of modules of all subjects recovered at a threshold of 1.3 is shown in

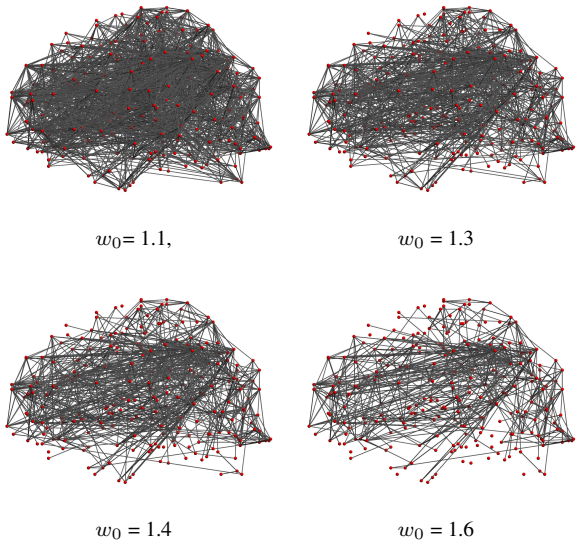


**Fig. 2**: Functional brain networks of a representative subject at different thresholds $w_0$ of functional connectivity.

the histogram for standard and degree-corrected block models figure 4.

As seen, standard and degree-corrected block models give different numbers of modules for different subjects. At connectivity threshold of 1.3, the SBM favored 3 modules while dc-SBM favored 6 modules. By visual inspection, the functional modules detected were similar to those obtained by modularity maximization algorithm [22].

## 4. DISCUSSION AND CONCLUSION

We fit network models based on degree distributions and weight distributions to rs-fMRI scans gathered in the HCP. The functional connectivity of the brain was calculated as partial correlations of fMRI time-series on 264 cortical ROI earlier identified as functionally relevant. The functional connectivity matrices had to be thresholded in order to evaluate goodness-of-fit of network models on brain scans. We investigated two types of network models: networks that are defined by distribution of (i) node degree and (ii) connection weights.

By applying rs-fMRI scans on a database of 627 subjects, we showed the validity of several network models on functional brain networks. Our results confirm that the two types of network models, those defined on degree distribution and those defined on connectivity distribution, capture different aspects of network topology. This supports our hypothesis that brain networks have the tendency to organize network topology into functional modules by preserving distribution of connection strength and the drive of brain networks to high topological integration by means of short communi-

**Table 2**: Log likelihood ratio, $\log(l_2/l_1)$, (x$10^3$) and $p$-values between different models computed on all scans at the connectivity threshold of 1.3

| log ($l_2$/ $l_1$), $p$-value | Exponential | Power-law | Stretched | dc-SBM | SBM |
|---|---|---|---|---|---|
| Exponential | - | 36.75, $< 0.05$ | - | 2.22, $< 0.05$ | 2193.23, $< 0.05$ |
| Power Law | - | - | - | 2181.90, $< 0.05$ | 2156.47, $< 0.05$ |
| Stretched | 2.45, $< 0.05$ | 39.20, $< 0.05$ | - | 2221.10, $< 0.05$ | 2195.68, $< 0.05$ |
| dc-SBM | - | - | - | - | - |
| SBM | - | - | - | 25422, $< 0.05$ | - |

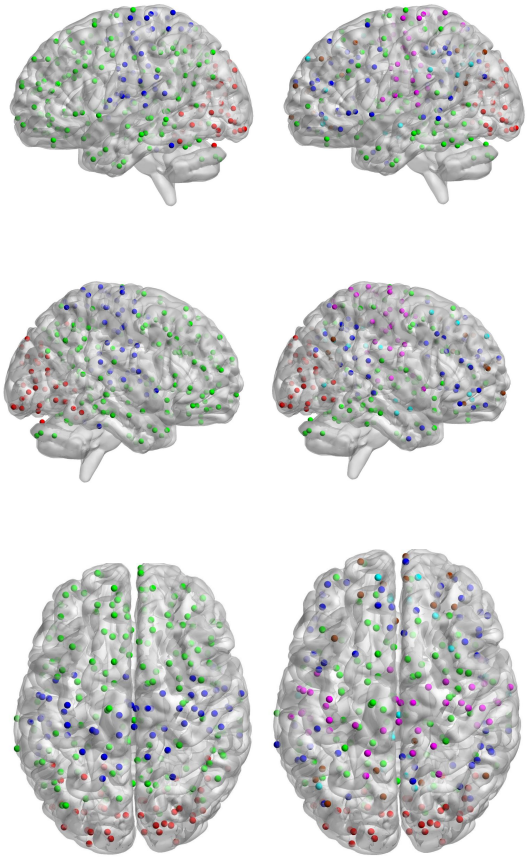

**Fig. 3**: Modules in the functional brain network for a representative subject for degree-corrected (on left) and non-degree corrected (on right) stochastic block model at connectivity-theshold of 1.3: top row are sagittal left views; middle are sagittal right views; and bottom row are axial top view.

cation paths, hubs and rich hubs by networks preserving the networks of nodal distribution.

Our study should help to understand how the brain organization compromise to have an architecture between small world networks and modular networks. As a future of this work, individual variability of different models across subjects can be studied. Further, thresholding step of connectivity need to be avoided by using analysis based on weighted networks.

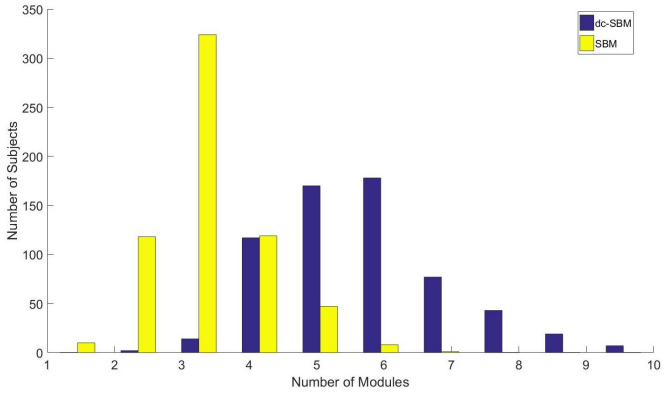


**Fig. 4**: Number of modules detected at threshold 1.3

## 5. ACKNOWLEDGMENT

This work was partially supported by AcRF Tier 1 grant RG 19/15 of Ministry of Education, Singapore. Data were provided [in part] by the Human Connectome Project, WU-Minn Consortium (Principal Investigators: David Van Essen and Kamil Ugurbil; 1U54MH091657) funded by the 16 NIH Institutes and Centers that support the NIH Blueprint for Neuroscience Research; and by the McDonnell Center for Systems Neuroscience at Washington University.

## 6. REFERENCES

[1] M. F. Glasser, et al., "A multi-modal parcellation of human cerebral cortex," Nature, 2016, vol. 536, no. 7615, pp. 171-178

[2] D. Meunier et al., "Modular and Hierarchically Modular Organization of Brain Networks," Frontiers in Neuroscience, 2010, vol. 4, pp. 1-11

[3] O. Sporns and R. F. Betzel. "Modular brain networks," Annu Rev Psychol., 2016, vol. 67(1): 613-640

[4] C. J. Stam, "Modern network science of neurological disorders," Nature Reviews Neuroscience, 2014, vol. 15, no. 10, pp. 683-695

[5] M. P. van den Heuvel, et al., Comparative Connectomics, Trends in Cognitive Sciences, 2016, vol. 20, no. 5, pp. 345–361

[6] D. S. Bassett and E. D. Bullmore, "Small-world brain networks." The Neuroscientist, 2006, vol. 12, no. 1, pp. 512-523.

[7] S. Achard et al., "A resilient, low-frequency, small-world human brain functional network with highly connected association cortical hubs." The Journal of neuroscience 2006, vol. 26, no. 1, pp. 63-72

[8] D. Meunier et al., "Age-related changes in modular organization of human brain functional networks," NeuroImage, 2009, vol. 44, 3, pp. 715–723

[9] D. S. Bassett, "Dynamic reconfiguration of human brain networks during learning," Proceedings of the National Academy of Sciences, 2011, pp. 1–6

[10] M. Rubinov and O. Sporns, "Weight-conserving characterization of complex functional brain networks," NeuroImage, 2011, vol. 56, no. 4, pp. 2068–2079,

[11] B. Karrer and M. E. J. Newman. "Stochastic blockmodels and community structure in networks." Physical Review E 83.1 (2011): 016107.

[12] D. C. Van Essen et al., " The Human Connectome Project: A data acquisition perspective," NeuroImage, 2012, vol. 62, no. 4, pp. 2222–2231

[13] T. P. Peixoto, "Entropy of stochastic blockmodel ensembles, Physical Review. E, Statistical, nonlinear, and soft matter physics, 2012, vol. 85, no. 5 Pt 2, pp. 056122,

[14] T. P. Peixoto, "Efficient Monte Carlo and greedy heuristic for the inference of stochastic block models." Physical Review E 89.1 (2014): 012804.

[15] J. D. Power et al., "Functional network organization of the human brain," Neuron, 2011, vol. 72(4): 665-678

[16] R. Albert and A. Barabási, "Statistical mechanics of complex networks," Reviews of Modern Physics, 2002, 74:1, pp. 47–97

[17] A Clauset et al., "Power-law distributions in empirical data," arXiv.org, 2007, no. 4, pp. 661–703

[18] L. A. Amaral et al., "Classes of small-world networks," Proceedings of the National Academy of Sciences of the United States of America, 2000, 97:21, pp. 11149–11152,

[19] J. Alstott et al., "powerlaw: a Python package for analysis of heavy-tailed distributions," PloS one 9.1 (2014): e85777.

[20] M. F. Glasser et al., "The minimal preprocessing pipelines for the Human Connectome Project," NeuroImage, 2013, 80:C, pp. 105–124

[21] G. Salimi-Khorshidi et al., Automatic denoising of functional MRI data: Combining independent component analysis and hierarchical fusion of classifiers, NeuroImage, 2014, vol. 90, pp. 449–468

[22] M. W. Cole et al., "Intrinsic and Task-Evoked Network Architectures of the Human Brain," Neuron, 2014,83:1, pp. 238–251

[23] Q. H. Vuong, "Likelihood ratio tests for model selection and non-nested hypotheses," Econometrica: Journal of the Econometric Society (1989): 307-333.

[24] Tiago P. Peixoto, The graph-tool python library, figshare. (2014) DOI: 10.6084/m9.figshare.1164194